

## Studies on the Biosynthesis of Paraherquamide A and VM99955. A Theoretical Study of Intramolecular Diels–Alder Cycloaddition

Luis R. Domingo,\* Ramón J. Zaragoza, and Robert M. Williams<sup>§</sup>

*Instituto de Ciencia Molecular, Departamento de Química Orgánica, Universidad de Valencia, Dr. Moliner 50, E-46100 Burjassot, Valencia, Spain, and Department of Chemistry, Colorado State University, Fort Collins, Colorado 80523*

domingo@utopia.uv.es

Received August 26, 2002

Intramolecular Diels–Alder reactions of 2-azadiene models have been studied quantum chemically at the B3LYP/6-31G\* level in order to elucidate the stereochemical features of the cyclization step involved in the biosynthesis of paraherquamide A and VM99955. These cycloadditions take place through concerted transition states associated with [4 + 2] processes. Analysis of the energies along the competitive paths reveals that while the cycloadditions of the oxindoles present a large anti selectivity, the indoles show a low syn selectivity for the formation of the C20 stereogenic center that is larger for the reduced tertiary amide form. The presence of the C14 methyl of the  $\beta$ -methylproline ring produces a low hindrance along the reaction coordinate for the syn approach of the isoprene framework, in agreement with the low facial selectivity found experimentally. An analysis of the electrophilicity and activation parameters for experimental models of the inter- and intramolecular Diels–Alder reactions reveals several significant factors controlling these biosynthetic cyclizations. The results are in reasonable agreement with the available experimental data.

### 1. Introduction

Paraherquamides<sup>1</sup> (e.g., paraherquamide A (**1**)), VM55599 (**2**),<sup>2</sup> brevianamides<sup>3</sup> (e.g., brevianamide A (**3**), brevianamide B (**4**)), marcfortines,<sup>4</sup> and sclerotamide<sup>5</sup> are indolic secondary metabolites isolated from various fungi. They have attracted considerable attention due to their molecular complexity, intriguing biogenesis, and some for members, most notably the paraherquamides, for their

potent antiparasitic activity. These alkaloids share an unusual bicyclo[2.2.2]diazaoctane ring system that has been proposed to arise via an intramolecular Diels–Alder cycloaddition of the isoprene double bond across the  $\alpha$ -carbons of the amino acid subunits, as depicted in Scheme 2.<sup>6,7</sup>

In 1993, Everett and co-workers isolated VM55599 (**2**), a very minor metabolite that also possesses the bicyclo[2.2.2]diazaoctane core, from the same *Penicillium* sp. that produces paraherquamide A (**1**).<sup>2</sup> On the basis of the structural similarities of these cometabolites, Everett et al. speculated that VM55599 might be a biosynthetic precursor to paraherquamide A.<sup>2</sup> The stereochemistry of the methyl group in the  $\beta$ -methylproline ring was assigned as being syn to the bridging isoprene moiety. In all other known members of the paraherquamide family, this methyl group is positioned in an anti arrangement.

\* Universidad de Valencia.

<sup>§</sup> Colorado State University.

(1) (a) Yamakazi, M.; Okuyama, E.; Kobayashi, M.; Inoue, H. *Tetrahedron Lett.* **1981**, *22*, 135–136. (b) Ondeyka, J. G.; Goegelman, R. T.; Schaeffer, J. M.; Kelemen, L.; Zitano, L. *J. Antibiot.* **1990**, *43*, 1375–1379. (c) Liesch, J. M.; Wichmann, C. F. *J. Antibiot.* **1990**, *43*, 1380–1386. (d) Blanchflower, S. E.; Banks, R. M.; Everett, J. R.; Manger, B. R.; Reading, C. *J. Antibiot.* **1991**, *44*, 492–497. (e) Banks, R. M.; Blanchflower, S. E.; Everett, J. R.; Manger, B. R.; Reading, C. *J. Antibiot.* **1997**, *50*, 840–846.

(2) Blanchflower, S. E.; Banks, R. M.; Everett, J. R.; Reading, C. *J. Antibiot.* **1993**, *46*, 1355–1363.

(3) (a) Birch, A. J.; Wright, J. J. *J. Chem. Soc., Chem. Commun.* **1969**, 644–645. (b) Birch, A. J.; Wright, J. J. *Tetrahedron* **1970**, *26*, 2329–2344. (c) Birch, A. J.; Rusell, R. A. *Tetrahedron* **1972**, *28*, 2999–3008. (d) Bird, B. A.; Remaley, A. T.; Campbell, I. M. *Appl. Environ. Microbiol.* **1981**, *42*, 521–525. (e) Bird, B. A.; Campbell, I. M. *Appl. Environ. Microbiol.* **1982**, *43*, 345. (f) Robbers, J. E.; Straus, J. W. *Lloydia* **1975**, *38*, 355. (g) Paterson, R. R. M.; Hawksworth, D. L. *Trans. Br. Mycol. Soc.* **1985**, *85*, 95–100. (h) Wilson, B. J.; Yang, D. T. C.; Harris, T. M. *App. Microbiol.* **1973**, *26*, 633–635. (i) Coetzer, J. *Acta Crystallogr., Sect. B* **1974**, *30*, 2254–2256.

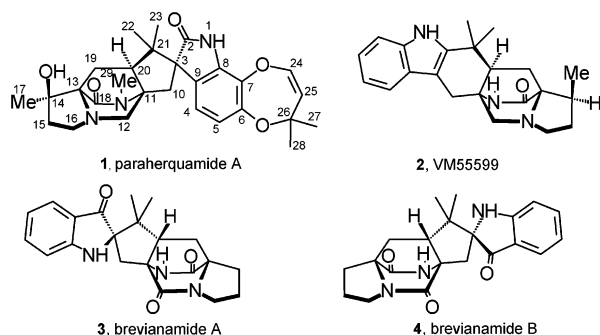
(4) (a) Polonsky, J.; Merrien, M.-A.; Prangé, T.; Pascard, C. *J. Chem. Soc., Chem. Commun.* **1980**, 601–602. (b) Prangé, T.; Billion, M.-A.; Vuilhorgne, M.; Pascard, C.; Polonsky, J. *Tetrahedron Lett.* **1980**, *22*, 1977–1980.

(5) Whyte, A. C.; Gloer, J. B.; Wicklow, D. T.; Dowd, P. F. *J. Nat. Prod.* **1996**, *59*, 1093–1095.

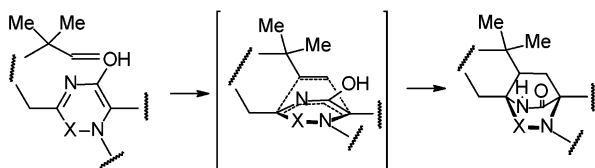
(6) (a) Porter, A. E. A.; Sammes, P. G. *J. Chem. Soc., Chem. Commun.* **1970**, 1103. (b) Williams, R. M.; Kwast, E.; Coffman, H.; Glinka, T. *J. Am. Chem. Soc.* **1989**, *111*, 3064–3065. (c) Williams, R. M.; Glinka, T.; Kwast, E.; Coffman, H.; Stille, J. K. *J. Am. Chem. Soc.* **1990**, *112*, 808–821. (d) Sanz-Cervera, J. F.; Glinka, T.; Williams, R. M. *J. Am. Chem. Soc.* **1993**, *115*, 347–348. (e) Sanz-Cervera, J. F.; Glinka, T.; Williams, R. M. *Tetrahedron* **1993**, *49*, 8471–8482. (f) Stocking, E. M.; Sanz-Cervera, J. F.; Williams, R. M. *Angew. Chem., Int. Ed.* **1999**, *38*, 786–789.

(7) (a) Williams, R. M.; Sanz-Cervera, J. F.; Sancenón, F.; Marco, J. A.; Halligan, K. *J. Am. Chem. Soc.* **1998**, *120*, 1090–1091. (b) Stocking, E. M.; Sanz-Cervera, J. F.; Williams, R. M. *J. Am. Chem. Soc.* **2000**, *122*, 1675–1683. (c) Sanz-Cervera, J. F.; Williams, R. M. *J. Am. Chem. Soc.* **2002**, *124*, 2556–2559. (d) Stocking, E. M.; Sanz-Cervera, J. F.; Williams, R. M. *Angew. Chem., Int. Ed.* **2001**, *40*, 1296–1298.

## SCHEME 1



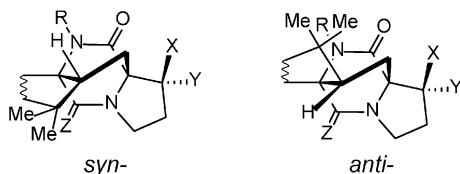
## SCHEME 2



Recently, Williams et al. have proposed an unified biogenesis of the paraherquamides and VM55599 as shown in Scheme 3.<sup>7</sup> All the metabolites are invoked to result from an intramolecular Diels–Alder cycloaddition of a common azadiene, **5**, through two (see **a** and **b** in Scheme 3, *syn*-selective) of the four possible diastereoisomeric transition states **a–d**.<sup>8</sup> If the cycloaddition occurs with the methyl group of the  $\beta$ -methylproline ring anti to the isoprene unit (as in **a** in Scheme 3), the intermediates **6** or **7** would be formed, which would lead to all of the paraherquamides containing a  $\beta$ -methylproline moiety. A minor shunt pathway would involve cycloaddition from the face of the azadiene with the methyl group of the  $\beta$ -methylproline ring *syn* to the isoprene unit (see **b** in Scheme 3) and VM55599 (**2**) or its oxidized analogue **8** would thus result.<sup>9</sup> On the other hand, cycloadducts **9** and **10**, resulting from anti disposition of the isoprene double bond relative to the azadiene, would lead to the corresponding C20-*epi*-metabolites thus far not detected in the paraherquamide-producing fungi. However, the anti relative stereochemistry is observed in brevianamides A (**3**) and B (**4**).

This hypothesis has been recently tested through feeding experiments with doubly <sup>13</sup>C-labeled compounds **2** and **6–8**.<sup>7d</sup> These experiments revealed that only intermediate **6** was incorporated into paraherquamide A (**1**), while racemic, doubly <sup>13</sup>C-labeled VM55599 (**2**), **7**, and **8** were not incorporated. These experiments suggest

(8) *Syn/anti* relationship refers to the relative stereochemistry between the C20 stereogenic center (paraherquamide A numbering) and the cyclic amino acid residue (proline or  $\beta$ -methylproline).



(9)  $\alpha/\beta$  facial selectivity for the cyclization of the C14 methyl derivative **5** refers to the approach of the isoprene unit from the same or the opposite face containing the C14 methyl group, to distinguish it from the *syn/anti* selectivity in the formation of the C20 stereogenic center (see ref 8).

that the formation of the bicyclo[2.2.2]diazaoctane occurs at a stage wherein the indole portion of the tryptophyl moiety has not yet been oxidized.<sup>7d</sup> This mandates that oxidation of the indole ring to form the catechol derivative dioxepin and spirooxindole occurs after the formation of this intermediate. These results also cast considerable doubt on the intermediacy of VM55599 (**2**) and its oxidized analogue **8** in the biosynthesis of the paraherquamides and provide additional circumstantial evidence that VM55599 (**2**) is a minor shunt metabolite.

Several theoretical works devoted to the study of the aza-Diels–Alder reactions using 1-azabutadienes<sup>10</sup> and 2-azabutadienes<sup>11</sup> have been reported in the literature. Cycloadditions of 1-aza- and 2-aza-1,3-butadiene with ethylene present large barriers of 21.8<sup>10e</sup> and 21.7<sup>12</sup> kcal/mol (B3LYP/6-31G\* results), respectively. Therefore, the participation of simple azadienes in normal [4 + 2] cycloaddition reactions with nonactivated dienophiles is rarely observed. However, this problem can be circumvented by introducing either electron-withdrawing or electron-donating substituents onto the nitrogen atom.

A recent theoretical study of an indoxyl-based aza-Diels–Alder cyclization pathway supported the observed isomer distribution of the brevianamides in *Penicillium brevicompactum*, which produces brevianamide A (**3**) as the major metabolite and brevianamide B (**4**) as the minor metabolite; both natural products possess the anti relationship.<sup>13</sup> The *syn* isomers were found to have a larger activation energy in agreement with the fact that the corresponding indoxyl-based natural products are unknown. The constraints imposed at the stage of the five-membered ring-formation in these intramolecular cycloadditions were found to be responsible for the large anti selectivity observed in the biosynthesis of the brevianamides.<sup>13</sup> This intermolecular aza-Diels–Alder reaction presents a large barrier, 22.6 kcal/mol (MP3/6-31G\*\*/HF/6-31G\* results).

In the present work, a density functional theory (DFT) study of the intramolecular cycloaddition reaction allowing the formation of the *syn* bicyclo[2.2.2]diazaoctane ring system present in paraherquamide A (**1**) and VM55599 (**2**) was carried out in order to elucidate the stereochemically determining features of the cyclization step and the factors controlling the activation parameters for these biosynthetic aza-Diels–Alder reactions. Some inquiries were raised that the present study aims to address: (i) What is the *syn/anti* selectivity in the formation of the C20 stereogenic center at the indole or oxindole stage?

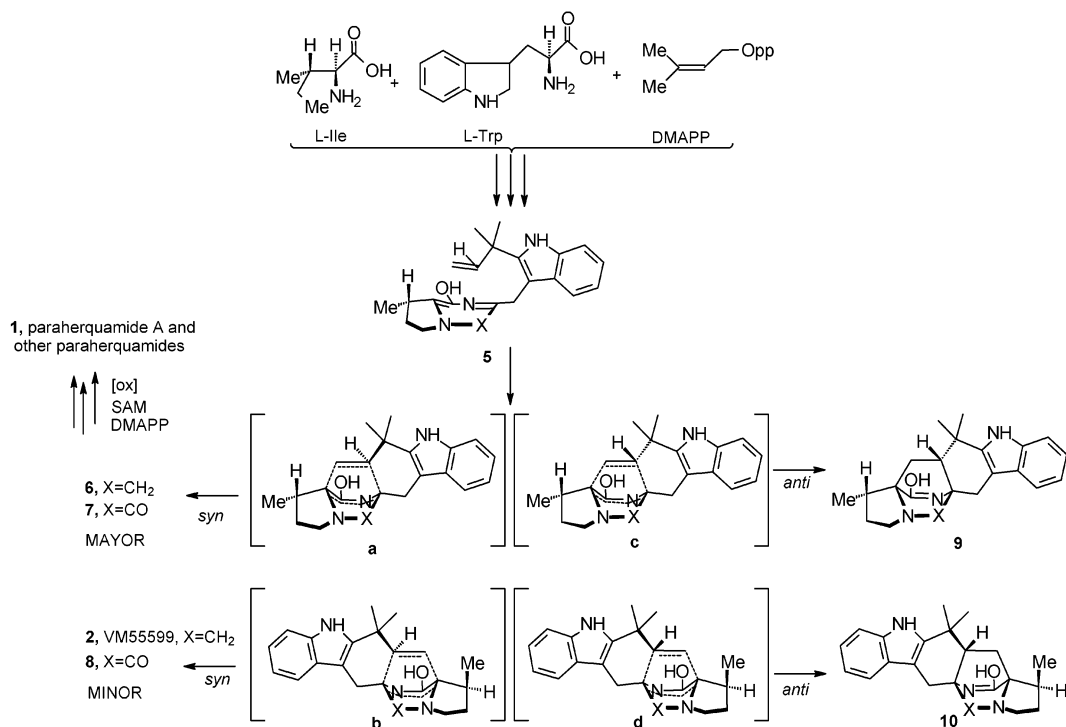
(10) (a) Boger, D. L.; Corbett, W. L.; Curran, T. T.; Kasper, A. M. *J. Am. Chem. Soc.* **1991**, *113*, 1713–1729. (b) Trần Hữu Dâu, M. E.; Flament, J.-P.; Lefour, J.-M.; Riche, C.; Grierson, D. S. *Tetrahedron Lett.* **1992**, *33*, 2343–2346. (c) Bachrach, S. M.; Liu, M. *J. Org. Chem.* **1992**, *57*, 6736–6744. (d) Tietze, L. F.; Fennen, J.; Geissler, H.; Schulz, G.; Anders, E. *Liebigs Ann.* **1995**, 1681–1687. (e) Park, Y. S.; Lee, B.-S.; Lee, I. *New J. Chem.* **1999**, *23*, 707–715. (f) Domingo, L. R. *Tetrahedron* **2002**, *58*, 3765–3774.

(11) (a) González, J.; Houk, K. N. *J. Org. Chem.* **1992**, *57*, 3031–3037. (b) Barluenga, J.; Sordo, T. L.; Sordo, J. A.; Fustero, S.; González, J. *J. Mol. Struct. (THEOCHEM)* **1994**, *315*, 63–69. (c) Venturini, A.; Joglar, J.; Fustero, S.; González, J. *J. Org. Chem.* **1997**, *62*, 3919–3926. (d) Pinho e Melo, T. M. V. D.; Fausto, R.; Rocha Gonsalves, A. M. D.; Gilchrist, T. L. *J. Org. Chem.* **1998**, *63*, 5350–5355. (e) Augusti, R.; Gozzo, F. C.; Moraes, L. A. B.; Sparrapan, R.; Eberlin, M. N. *J. Org. Chem.* **1998**, *63*, 4889–4897.

(12) Avalos, M.; Babiano, R.; Clemente, F. R.; Cintas, P.; Gordillo, R.; Jiménez, J. L.; Palacios, J. C. *J. Org. Chem.* **2000**, *65*, 8251–8259.

(13) Domingo, L. R.; Sanz-Cervera, J. F.; Williams, R. M.; Picher, M. T.; Marco, J. A. *J. Org. Chem.* **1997**, *62*, 1662–1667.

## SCHEME 3



(ii) What is the influence of the tertiary amide carbonyl or its reduced form on the stereochemistry of these cycloadditions? (iii) What is the facial selectivity for the C14 methyl derivatives?

## 2. Model Equations

The global electrophilicity power has been recently defined by Parr et al.<sup>14</sup>

$$\omega = \frac{\mu^2}{2\eta} \quad (1)$$

which measures the stabilization energy when the system acquires an additional electronic charge  $\Delta N$  from the environment. In eq 1,  $\mu$  and  $\eta$  are the electronic chemical potential and the chemical hardness of the ground state (GS) of atoms and molecules, respectively. These descriptors have been defined within the context of the density functional theory of Parr, Pearson, and Yang.<sup>15</sup> While the electronic chemical potential  $\mu$  describes the charge-transfer pattern of the system in its ground-state geometry, the chemical hardness describes the resistance to the change. A very simple operational formula for  $\mu$ , in terms of the one-electron energies of the frontier molecular orbitals HOMO and LUMO,  $\epsilon_H$  and  $\epsilon_L$ , respectively, is given by the following:<sup>15a</sup>

$$\mu \approx \frac{\epsilon_H + \epsilon_L}{2} \quad (2)$$

It is also possible to give a quantitative representation to the chemical hardness concept introduced by Pearson:<sup>15b</sup>

$$\eta \approx \epsilon_L - \epsilon_H \quad (3)$$

Note that the electrophilicity index given in eq 1 encompasses simultaneously both the propensity of the electrophile to acquire an additional electronic charge driven by  $\mu^2$  and the resistance of the system to exchange electronic charge with the environment described by  $\eta$ . A high value of  $\mu$  and a low value of  $\eta$  therefore characterize a good electrophile.

Associated with the definition of global electrophilicity, there is an additional and useful relationship that accounts for the maximum electronic charge  $\Delta N_{\max}$  that the electrophile may accept from the environment.<sup>14</sup>

$$\Delta N_{\max} = -\frac{\mu}{\eta} \quad (4)$$

Domingo and Contreras et al.<sup>16a</sup> have recently used the electrophilicity power for a series of dienes and dienophiles involved in Diels–Alder reactions to investigate the electronic nature of the transition structures (TS) involved in the Diels–Alder cycloadditions. They found that small differences between the electrophilicity,  $\Delta\omega$ , for the diene/dienophile pair can be correlated with nonpolar mechanisms (pericyclic processes), while large electrophilicity differences can be related to polar mechanisms (ionic processes).<sup>16a</sup> In addition, the electrophilicity

(14) Parr, R. G.; von Szentpály, L.; Liu, S. *J. Am. Chem. Soc.* **1999**, *121*, 1922–1924.

(15) (a) Parr, R. G.; Yang, W. *Density Functional Theory of Atoms and Molecules*; Oxford University Press: New York, 1989. (b) Parr, R. G.; Pearson, R. G. *J. Am. Chem. Soc.* **1983**, *105*, 7512–7516.

(16) (a) Domingo, L. R.; Aurell, M. J.; Pérez, P.; Contreras, R. *Tetrahedron* **2002**, *58*, 4417–4423. (b) Domingo, L. R.; Arnó, M.; Contreras, R.; Pérez, P. *J. Phys. Chem. A* **2002**, *106*, 952–961. (c) Domingo, L. R.; Aurell, M. J. *J. Org. Chem.* **2002**, *67*, 959–965. (d) Domingo, L. R.; Asensio, A.; Arroyo, P. *J. Phys. Org. Chem.* **2002**, *15*, 660–666.

licity for a series of the reagents involved in cycloaddition reactions can also be used to study the effects of the structural changes on reactivity.<sup>16</sup> Thus, it has been used to explain the reactivity of 1-azadiene derivatives on the inverse-electron-demand Diels–Alder reaction.<sup>10f</sup>

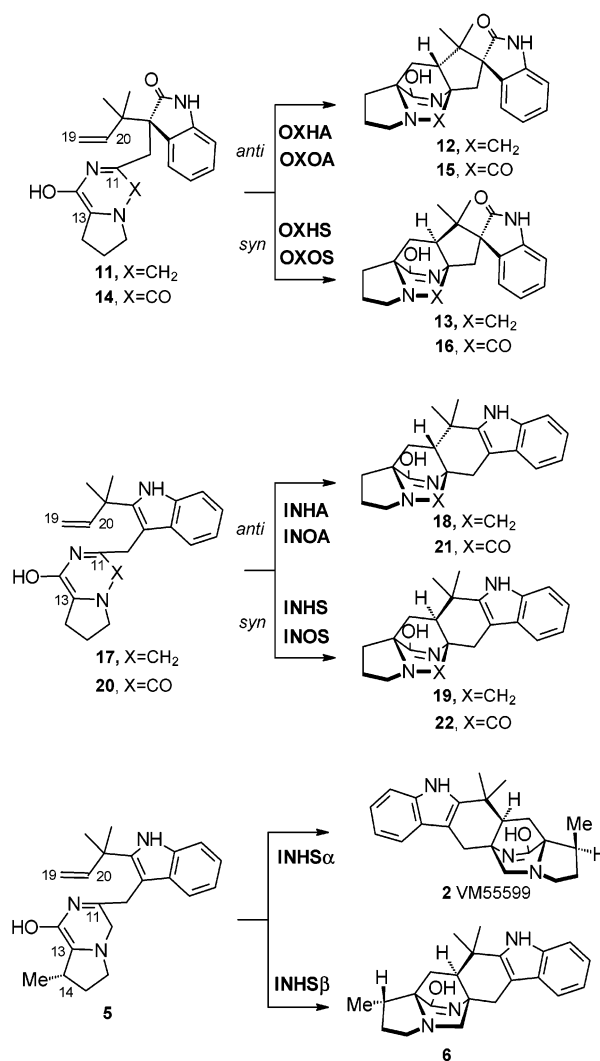
### 3. Computational Methods

An extensive exploration of the potential energy surface (PES) for these cycloadditions was first carried out at the HF/3-21G computational level.<sup>17</sup> Previous theoretical studies on Diels–Alder reactions and related pericyclic reactions indicated that the activation energies calculated at the HF level are too large, while DFT calculations using the B3LYP hybrid functional<sup>18</sup> have been shown to be in good agreement with experimental values.<sup>19</sup> Therefore, the HF stationary points were optimized and characterized at the B3LYP/6-31G\* level. The optimizations were carried out using the Bery analytical gradient optimization method.<sup>20</sup> The electronic structures of stationary points were analyzed by the natural bond orbital (NBO) method.<sup>21</sup> The bond order (BO) values have been evaluated using the Wiberg indexes.<sup>22</sup> The stationary points were characterized by frequency calculations in order to verify that the TSs have one and only one imaginary frequency.

The values of the relative enthalpies, entropies, and free energies have been calculated on the basis of the total energies and the thermochemical analysis at the B3LYP/6-31G\* level. The thermal contributions to the vibrational energy and entropy have been scaled by 0.96.<sup>23</sup> The energies have been computed at 25 °C, and the enthalpies and entropies were calculated with the standard statistical thermodynamic formulas.<sup>17</sup>

The global indices, electronic chemical potential  $\mu$ , chemical hardness  $\eta$ , and global electrophilicity  $\omega$ , defined in the context of DFT, have been evaluated from HOMO and LUMO energies of the reactants at the GS, at the same level of theory. All calculations were carried out with the Gaussian 98 suite of programs.<sup>24</sup>

### SCHEME 4



(17) Hehre, W. J.; Radom, L.; Schleyer, P. v. R.; Pople, J. A. *Ab initio Molecular Orbital Theory*; Wiley: New York, 1986.

(18) (a) Becke, A. D. *J. Chem. Phys.* **1993**, *98*, 5648–5652. (b) Lee, C.; Yang, W.; Parr, R. G. *Phys. Rev. B* **1988**, *37*, 785–789.

(19) (a) Stanton, R. V.; Merz, K. M., Jr. *J. Chem. Phys.* **1994**, *100*, 434–443. (b) Carpenter, J. E.; Sosa, C. P. *J. Mol. Struct. (THEOCHEM)* **1994**, *311*, 325–330. (c) Baker, J.; Muir, M.; Andzelm, J. *J. Chem. Phys.* **1995**, *102*, 2036. (d) Goldstein, E.; Beno, B.; Houk, K. N. *J. Am. Chem. Soc.* **1996**, *118*, 6036–6043. (e) Sbai, A.; Branchadell, V.; Ortuño, R. M.; Oliva, A. *J. Org. Chem.* **1997**, *62*, 3049–3054. (f) Wiest, O.; Montiel, D. C.; Houk, K. N. *J. Phys. Chem. A* **1997**, *101*, 8378–8388. (g) Tietze, L. F.; Pfeiffer, T.; Schuffenhauer, A. *Eur. J. Org. Chem.* **1998**, 2733–2741. (h) Domingo, L. R.; Arnó, M.; Andrés, J. *J. Org. Chem.* **1999**, *64*, 5867–5875.

(20) (a) Schlegel, H. B. *J. Comput. Chem.* **1982**, *3*, 214. (b) Schlegel, H. B. Geometry Optimization on Potential Energy Surface. In *Modern Electronic Structure Theory*; Yarkony, D. R., Ed.; World Scientific Publishing: Singapore, 1994.

(21) (a) Reed, A. E.; Weinstock, R. B.; Weinhold, F. *J. Chem. Phys.* **1985**, *83*, 735–746. (b) Reed, A. E.; Curtiss, L. A.; Weinhold, F. *Chem. Rev.* **1988**, *88*, 899–926.

(22) Wiberg, K. B. *Tetrahedron* **1968**, *24*, 1083–1096.

(23) Scott, A. P.; Radom, L. *J. Phys. Chem.* **1996**, *100*, 16502–16513.

(24) Frisch, M. J.; Trucks, G. W.; Schlegel, H. B.; Scuseria, G. E.; Robb, M. A.; Cheeseman, J. R.; Zakrzewski, V. G.; Montgomery, J. A., Jr.; Stratmann, R. E.; Burant, J. C.; Dapprich, S.; Millam, J. M.; Daniels, A. D.; Kudin, K. N.; Strain, M. C.; Farkas, O.; Tomasi, J.; Barone, V.; Cossi, M.; Cammi, R.; Mennucci, B.; Pomelli, C.; Adamo, C.; Clifford, S.; Ochterski, J.; Petersson, G. A.; Ayala, P. Y.; Cui, Q.; Morokuma, K.; Malick, D. K.; Rabuck, A. D.; Raghavachari, K.; Foresman, J. B.; Cioslowski, J.; Ortiz, J. V.; Stefanov, B. B.; Liu, G.; Liashenko, A.; Piskorz, P.; Komaromi, I.; Gomperts, R.; Martin, R. L.; Fox, D. J.; Keith, T.; Al-Laham, M. A.; Peng, C. Y.; Nanayakkara, A.; Gonzalez, C.; Challacombe, M.; Gill, P. M. W.; Johnson, B. G.; Chen, W.; Wong, M. W.; Andres, J. L.; Head-Gordon, M.; Replogle, E. S.; Pople, J. A. *Gaussian 98*, revision A.6; Gaussian, Inc.: Pittsburgh, PA, 1998.

### 4. Results and Discussion

**(i) Energies.** Five complete models were chosen to study the intramolecular cycloaddition step involved in the biosynthesis of paraherquamide A (**1**) and VM55599 (**2**). These models are related with respect to the anti and syn relationships for the formation of the C20 stereogenic center for the intramolecular cycloadditions at the oxindole stage **11** ( $X = \text{CH}_2$ ) and **14** ( $X = \text{CO}$ ), at the indole stage **17** ( $X = \text{CH}_2$ ) and **20** ( $X = \text{CO}$ ), and also with respect to the facial selectivity<sup>9</sup> of the cyclization of the C14 methyl indole **5**. A schematic representation for these intramolecular cycloadditions, including the atom numbering, is given in Scheme 4. Ten TSs, **OXHS**, **OXHA**, **OXOS**, **OXOA**, **INHS**, **INHA**, **INOS**, **INOA**, **INHS $\alpha$** , and **INHS $\beta$**  and their corresponding cycloadducts, were located and characterized. These acronyms are related to the oxindole and indole structures, named **OX** and **IN**, respectively, the reduced form of the tertiary amide (tertiary amine) or the tertiary amide, named **H** or **O**, respectively, and the syn or anti relationship for the formation of the C20 stereogenic center, named **S** or **A**, respectively. Finally, the facial selectivities for the approach of the isoprene moiety to both faces of the azadiene system of the C14 methylproline derivative **5**

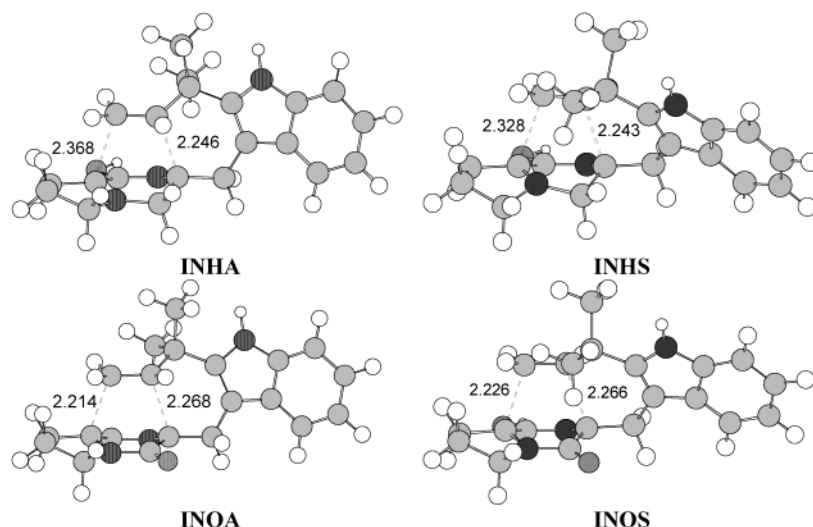


**FIGURE 1.** Transition structures corresponding to the cyclization of indoles **17** and **20**. Bond lengths directly involved in the reaction obtained at the B3LYP/6-31G\* level are given in Å.

**TABLE 1.** B3LYP/6-31G\* Relative Energies<sup>a</sup> (kcal/mol) for the Stationary Points Corresponding to the Cyclization of 2-Azadines **5**, **17**, and **20**

<b>5</b>	$\Delta E$	<b>17</b>	$\Delta E$	<b>20</b>	$\Delta E$
<b>INHS<math>\alpha</math></b>	24.9	<b>INHA</b>	25.2	<b>INOA</b>	27.0
<b>INHS<math>\beta</math></b>	24.8	<b>INHS</b>	24.1	<b>INOS</b>	26.8
<b>2</b>	-27.9	<b>18</b>	-30.1	<b>21</b>	-15.2
<b>6</b>	-27.6	<b>19</b>	-29.9	<b>22</b>	-15.7

<sup>a</sup> Relative to the corresponding 2-azadiene (**5**, **17**, or **20**).

are named  $\alpha$  (for the syn relationship) and  $\beta$  (for the anti relationship).<sup>9</sup> The total and relative energies of the stationary points involved in these intramolecular cycloadditions at different computational levels are given in Table 1S (see Supporting Information). The B3LYP/6-31G\* relative energies for the indole stage (**17** and **20**) and the C14 methylproline (**5**) are shown in Table 1. The HF geometries for the oxindole TSs are given in Figure 1S, while the B3LYP geometries of the TSs associated with the indoles **17** and **20** and the C14 methylproline **5** are shown in Figures 1 and 2.

A preliminary study for these cycloadditions at the B3LYP/6-31G\* // HF/3-21G level (see Table 1S) showed that for the oxindoles **11** (X = CH<sub>2</sub>) and **14** (X = CO), the anti reactive channels via **OXHA** and **OXOA** are clearly preferred over the syn reactive channels via **OXHS** and **OXOS** (by between 4 and 7 kcal/mol). These energies point out a large anti selectivity for the formation of the C20 stereogenic center, in disagreement with the syn relationship observed in the biosynthesis of paraherquamide (**1**) and VM55599 (**2**). Therefore, the large anti selectivity found for the cyclization of the oxindoles **11** and **14**, which is similar to that computed in the formation of the five-membered ring in the biosynthesis of brevianamides A (**3**) and B (**4**),<sup>13</sup> calls into question the possibility that the cycloaddition reaction occurs at the oxindole stage in the biosynthesis of paraherquamide A (**1**) and VM55599 (**2**).<sup>7d</sup> In view of this large anti selectivity, we decided not to perform the full optimizations for the oxindole stage at the DFT level.

An analysis of the relative energies (see Table 1) shows that these intramolecular cycloadditions present large

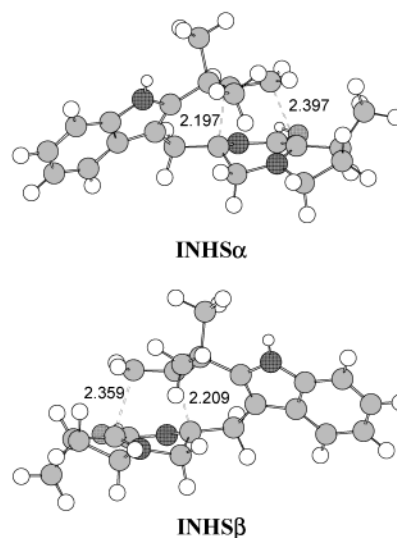


**FIGURE 2.** Transition structures corresponding to the cyclization of the 14 methyl derivative **5**. Bond lengths directly involved in the reaction obtained at the B3LYP/6-31G\* level are given in Å.

barriers, between 24.5 and 26.6 kcal/mol, which are even larger than that computed for the cycloaddition of 2-aza-1,3-butadiene and ethylene, 21.7 kcal/mol.<sup>12</sup>

The relative energies for the TSs involved in the syn/anti stereoselectivity for the formation of the C20 stereogenic center for the indoles **17** (X = CH<sub>2</sub>) and **20** (X = CO), **INHS**, **INHA**, **INOS**, and **INOA** indicate that the tertiary amide **20** presents a lower syn selectivity than the tertiary amine **17**; the syn **INHS** is 1.2 kcal/mol lower in energy than the anti **INHA**. These results are in reasonable agreement with the <sup>13</sup>C-labeling experiments carried out by Williams et al.,<sup>7b,c</sup> which concluded that the syn cycloaddition could take place via the nonoxidized tryptophyl moiety, and that the oxidation of the indole ring thus occurs after the cycloaddition.

Finally, an analysis of the relative energies associated with the facial selectivity for the intramolecular cycloaddition at the C14 methyl indole **5** shows that the

**TABLE 2.** Relative<sup>a</sup> Enthalpies (kcal/mol), Entropies (cal mol<sup>-1</sup> K<sup>-1</sup>), and Free Energies (kcal/mol) Calculated at 298.15 K and 1 atm for the Cyclization of 2-Azadines **5**, **17**, and **20**

	$\Delta H$	$\Delta S$	$\Delta G$
<b>INHSA</b>	24.7	-16.8	29.7
<b>INHSB</b>	24.5	-16.9	29.6
<b>2</b>	-25.1	-20.5	-19.0
<b>6</b>	-24.8	-21.8	-18.3
<b>INHA</b>	25.7	-7.9	29.1
<b>INHSA</b>	24.5	-9.5	28.6
<b>18</b>	-26.7	-12.1	-22.2
<b>19</b>	-26.4	-13.8	-21.8
<b>INOA</b>	26.6	-11.2	31.6
<b>INOS</b>	26.5	-13.7	31.5
<b>21</b>	-13.1	-14.9	-6.6
<b>22</b>	-13.7	-15.2	-7.6

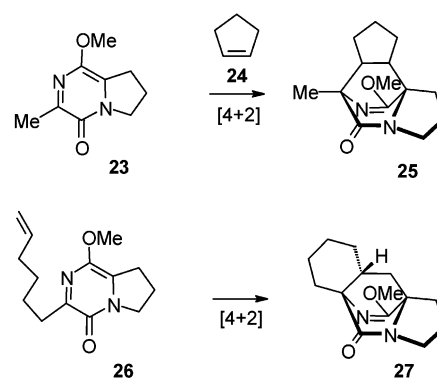
<sup>a</sup> Relative to the corresponding 2-azadiene (**5**, **17**, or **20**).

cycloaddition from the opposite face of the C14 methyl via **INHSA** is only 0.1 kcal/mol less energetically favorable than the attack from the same face via **INHSA**. This low facial selectivity, which agrees with experimental results,<sup>7b,c</sup> indicates that the C14 methyl group does not exert significant steric hindrance in these intramolecular cycloadditions. Therefore, the steric effect of the C14 methyl group is apparently not as important as originally had been thought in biasing the facial approach of the isoprene group.<sup>7c</sup>

The values of the relative enthalpies, entropies, and free energies for the intramolecular cycloadditions of indoles **5**, **17**, and **20** were also calculated. The energetic results are presented in Table 2. Inclusion of zero-point energy (ZPE) and the thermal contributions to the barriers does not modify substantially the activation enthalpies for the TSs. Thus, the activation enthalpies give a selectivity similar to that found in the previous analysis. The syn **INHSA** is 1.2 kcal/mol less energetically favorable than the anti **INHA**, while **INHSA** is only 0.2 kcal/mol more energetically favorable than **INHSA**. The activation entropies for these intramolecular cycloadditions range from -7.9 to -9.5 cal mol<sup>-1</sup> K<sup>-1</sup> for **17** to -16.8 to -16.9 cal mol<sup>-1</sup> K<sup>-1</sup> for **5**, the latter being similar to those computed for a reduced model for the intramolecular Diels-Alder reaction involved in the brevianamide biosynthesis, approximately -16 cal mol<sup>-1</sup> K<sup>-1</sup>.<sup>13</sup> Inclusion of the activation entropy raises the activation free energy for the complete model **5** to 29.6 kcal/mol. Inclusion of the activation entropies decreases the selectivities as a consequence of the larger relative negative entropy found at the more favorable TSs. Cyclizations involving the tertiary amine are very exergonic processes, between -18 and -21 kcal/mol.

**(ii) Geometries.** The lengths of the newly forming bonds C11-C20 and C13-C19 in structures **17** and **5** are 2.246 and 2.368 Å in **INHA**, 2.243 and 2.328 Å in **INHSA**, 2.197 and 2.397 Å in **INHSA**, and 2.209 and 2.359 Å in **INHSA**, respectively (Figures 1 and 2). The extent of the asynchronicity of the bond formation can be measured by means of the difference between the lengths of the  $\sigma$ -bonds that are being formed in these intramolecular cycloadditions, i.e.,  $\Delta r = d(\text{C13-C19}) - d(\text{C11-C20})$ . These values,  $\Delta r = 0.12$  for **INHA**,  $\Delta r = 0.09$  for **INHSA**,  $\Delta r = 0.20$  for **INHSA**, and  $\Delta r = 0.15$  for **INHSA**, indicate that these TSs correspond to the concerted

**SCHEME 5**



$\sigma$ -bond formation processes. In addition, the more favorable TSs are slightly less asynchronous. Thus, for the intramolecular cycloaddition of the C14 methyl indole **5**, **INHSA** is slightly more asynchronous than **INHSA** as a consequence of the slight increase of the C13-C19 length. The BO values of the two  $\sigma$ -bonds that are being formed at the indole TSs are between 0.37 and 0.39 for the C11-C20 bond formation and between 0.28 and 0.31 for the C13-C19 bond formation. These values that agree with the synchronicity obtained from the geometrical parameters indicate a concerted bond formation in the TSs.

An analysis of the TSs associated with the formation of the C20 stereogenic center for the indole **17** reveals that the newly forming six-membered ring containing the indole framework adopts a different arrangement in the anti and syn TSs. Thus, while in the more unfavorable anti **INHA**, this forming ring adopts a boat arrangement, whereas in the more favorable syn **INHSA**, it adopts a twist-boat arrangement. Therefore, the larger torsional energy associated with the boat conformation accounts for the larger energy for **INHA**. A different behavior was found in the intramolecular cycloadditions involved in the biosynthesis of the brevianamides **A** (**3**) and **B** (**4**) where the formation of the five-membered ring was found to be responsible for the large anti selectivity.<sup>13</sup>

**(iii) Analysis of Factors Controlling These Intramolecular aza-Diels-Alder Reactions.** The factors that influence the activation parameters of these biosynthetic intramolecular aza-Diels-Alder reactions have been analyzed. Sanz-Cervera and Williams et al.<sup>25</sup> have recently used some synthetic models for the [4 + 2] cycloaddition to gain additional insight into the biosynthesis of brevianamides, paraherquamides, and related compounds. Therefore, we have chosen two cycloadditions for which there are experimental data: the intermolecular [4 + 2] cycloaddition between the 2-azadiene **23**, in which the OMe group models the bulky O-BOC,<sup>25</sup> and cyclopentene **24** and the intramolecular [4 + 2] cycloaddition of compound **26** (see Scheme 5). The low reactivity of the 2-azadienes with the nonactivated dienophile was clearly noticeable. The intermolecular cycloaddition was done in the absence of a Lewis acid catalyst in ethyl acetate under pressure, at 100 °C and for a prolonged reaction time (45 h, yield 60%). In contrast, when

(25) Sanz-Cervera, J. F.; Williams, R. M.; Marco, J. A.; López-Sánchez, J. M.; González, F.; Martínez, M. E.; Sancenón, F. *Tetrahedron* **2000**, *56*, 6345-6358.

**TABLE 3.** Global Properties<sup>a</sup> of Some Dienes and Dienophiles

molecule	$\mu$	$\eta$	$\omega$
2-azadiene <b>23</b>	-0.1168	0.1455	1.28
2-aza-1,3-butadiene	-0.1325	0.2069	1.16
1,3-butadiene	-0.1270	0.2083	1.05
ethylene	-0.1239	0.2855	0.73
propene	-0.1108	0.2781	0.60
cyclopentene <b>24</b>	-0.0982	0.2676	0.49

<sup>a</sup> Electronic chemical potential,  $\mu$ , and chemical hardness,  $\eta$ , values are in au; electrophilicity power values,  $\omega$ , are in eV.

**TABLE 4.** Activation Parameters, Enthalpies (kcal/mol), Entropies (cal mol<sup>-1</sup> K<sup>-1</sup>), and Free Energies (kcal/mol), Calculated at 298.15 K and 1 atm for Some Diels–Alder Reaction Models

cycloaddition	$\Delta H^\ddagger$	$\Delta S^\ddagger$	$\Delta G^\ddagger$
butadiene/ethylene	24.1	-44.5	37.4
2-azadiene <b>23</b> /cyclopentene <b>24</b>	26.1	-46.6	40.0
2-azadiene <b>26-e</b>	24.4	-13.8	28.4
2-azadiene <b>26-f</b>	19.7	-11.9	23.3

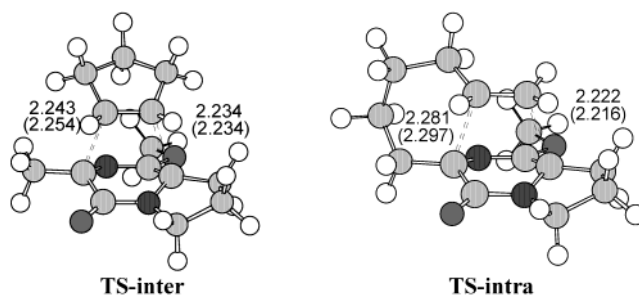
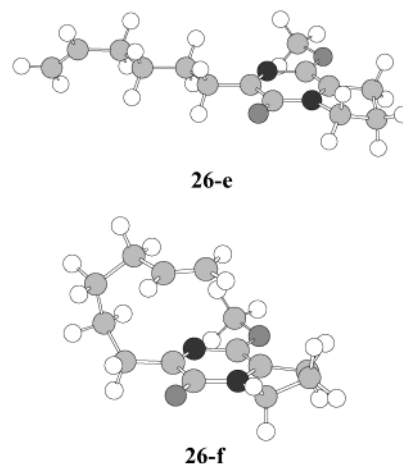
compound **26** was dissolved in THF and kept at room temperature for 15 h, it gave the cycloadduct **27** in 42% yield.<sup>25</sup>

The electronic features of these aza-Diels–Alder reactions have been analyzed using the global index defined on the DFT (see Model Equations section). The global properties, including the electrophilicity power of some reagents, are presented in Table 3. The electrophilicity of the 2-azadiene **23**,  $\omega = 1.28$  eV, is slightly larger than those for 2-aza-1,3-butadiene and 1,3-butadiene (1.16 and 1.05 eV, respectively). On the other hand, in the series ethylene, propene, as a model for the hexenyl chain present on 2-azadiene **26**, with cyclopentene, the electrophilicity decreases with the increase of the alkyl substitution on the ethylenic system as a consequence of the electron-releasing character of an alkyl substituent ( $\omega = 0.73, 0.64$ , and  $0.49$  eV, respectively).<sup>16b</sup>

The difference in electrophilicity,  $\Delta\omega$ , for the 2-azadiene **23**/cyclopentene and 2-azadiene **23**/propene pairs are 0.79 and 0.68 eV, respectively. These low values, which are slightly larger than those for the 1,3-butadiene/ethylene and 2-aza-1,3-butadiene/ethylene pairs ( $\Delta\omega = 0.32$  and  $0.42$  eV, respectively), indicate that these cycloadditions are associated with a nonpolar [4 + 2] process and provide an explanation for the low reactivity of these 2-azadienes.<sup>10f</sup> In addition, these low  $\Delta\omega$  values anticipate a low charge transfer at the corresponding TSs.<sup>16a,26</sup>

The activation parameters for the 2-azadiene **23**/cyclopentene cycloaddition and the cyclization of the 2-azadiene **26** have also been studied. Table 4 presents the energetic results, while Figure 4 shows the geometry of the TSs.

For the 2-azadiene **26**, two conformers have been considered. The less energetic one corresponds to the extended arrangement of the hexenyl chain (**26-e**), whereas the folded arrangement, which allows for the cyclization, is only 4.6 kcal/mol higher in energy (see **26-e** and **26-f** in Figure 4). The activation enthalpy for the

**FIGURE 3.** Transition structures corresponding to the intermolecular cycloaddition between the 2-azadiene **23** and cyclopentene **24**, **TS-inter**, and the cyclization of the 2-azadiene **26**, **TS-intra**. Bond lengths directly involved in the reaction obtained at the B3LYP/6-31G\* and B3LYP/6-31G\* levels in tetrahydrofuran (in parentheses) are given in Å.**FIGURE 4.** Geometries of the extended (**26-e**) and folding (**26-f**) conformations for the 2-azadiene **26**.

cyclization of **26-e** is 24.4 kcal/mol (19.7 kcal/mol from **26-f**) (see Table 4). This activation enthalpy is 1.7 kcal/mol lower than that for 2-azadiene **23**/cyclopentene intermolecular cycloadditions, which is 26.1 kcal/mol. These large values are in agreement with the low  $\Delta\omega$  for the diene/dienophile pairs involved in these nonpolar cycloadditions.

The [4 + 2] cycloadditions are entropically very unfavorable because of the geometry restrictions imposed on both TSs and cycloadducts. Thus, the butadiene/ethylene cycloaddition has an activation entropy of  $-44.5$  cal mol<sup>-1</sup> K<sup>-1</sup>, which raises the free energy of activation to 37.4 kcal/mol, rendering this intermolecular process very unfavorable (see Table 4).<sup>27</sup> A similar result is found for the intermolecular 2-azadiene **23**/cyclopentene cycloaddition where the computed free energy of activation increases to 40.0 kcal/mol.

However, a different result was found for the cyclization of the 2-azadiene **26**. For this intramolecular process, the negative activation entropy is only  $-13.8$  cal mol<sup>-1</sup> K<sup>-1</sup>, and as a consequence, the computed free energy of activation for the intramolecular mode is found to be 28.4 kcal/mol from **26-e** (23.3 kcal/mol from **26-f**, see Table

(26) Natural population analysis<sup>21</sup> indicates that the actual charge transfer at the **TS-inter** is negligible (0.02 e), in agreement with a nonpolar process.<sup>16a</sup>

(27) Diels–Alder reaction between butadiene and ethylene must be forced to take place: after 17 h at 165 °C and 900 atm, it does give a yield of 78%. Diels, O.; Alder, K. *Justus Liebigs Ann. Chem.* **1928**, 460, 98–122.

4). Therefore, the low activation free energy found for the intramolecular [4 + 2] process relative to the intermolecular one (40.0 kcal/mol) provides an explanation for the spontaneous cyclization of the 2-azadiene **26**<sup>25</sup> without the participation of any Lewis acid catalyst.<sup>28</sup>

The free energy of activation for the intramolecular cyclization of **5** (29.6 kcal/mol), which leads to the formation of VM55599 and paraherquamide A, is slightly larger than that found for the 2-azadiene **26**. However, the constraints imposed in the active site of the putative oxidase that forms the azadiene system from the diketopiperazine precursor can decrease both the enthalpy of activation by a reorganization of the folded conformation<sup>29</sup> and the favorable entropy of activation by an entropic trap,<sup>30</sup> favoring the cyclization process. Therefore, these cooperative factors, together with the lower free energy of activation found for the cyclization process, can permit these biosynthetic cyclizations to proceed without the formation of any covalent interactions at the active site.<sup>31</sup>

Finally, solvent effects on these aza-Diels–Alder reactions have been considered, optimizing the B3LYP/6-31G\* gas-phase stationary points corresponding to the experimental models, **23** + **24** and **26**, using a relatively simple self-consistent reaction field (SCRf) method<sup>32</sup> based on the polarizable continuum model of Tomasi's group.<sup>33</sup> The solvents used in the experiments were ethyl acetate,  $\epsilon = 6.08$ , and tetrahydrofuran,  $\epsilon = 7.58$ .<sup>25</sup> Therefore, we have used the dielectric constant of tetrahydrofuran at 298.0 K.

Inclusion of solvent effects stabilizes both reactants and TSs between 4.0 and 4.2 kcal/mol. The potential energy barriers are reduced on going from gas phase to tetrahydrofuran by 0.1 kcal/mol. This poor solvent effect can be attributed to the low polar character of these cycloadditions.<sup>26</sup> A comparison of the geometrical parameters of the TSs given in Figure 3 shows that the inclusion of solvent effects on the geometry optimization does not modify substantially the geometries obtained in the gas phase. Therefore, the inclusion of solvent effects on the experimental models does not alter the gas-phase analysis.

(28) Similar result has been found for the unfavorable [5 + 2] cycloaddition of  $\gamma$ -pyrones for which the lower negative activation entropy associated with the intramolecular process accounts for the facility of these cycloadditions. Domingo, L. R.; Zaragoza, R. J. *J. Org. Chem.* **2000**, *65*, 5480–5486.

(29) Cannon, W. R.; Benkovic, S. J. *J. Bio. Chem.* **1998**, *273*, 26257–26260.

(30) Villà, J.; Štrajbl, M.; Glennon, T. M.; Sham, Y. Y.; Chu, Z. T.; Warshel, A. *Proc. Natl. Acad. Sci. U.S.A.* **2000**, *97*, 11899–11904.

(31) Kim, S. P.; Leach, A. G.; Houk, K. N. *J. Org. Chem.* **2002**, *67*, 4250–4260.

(32) (a) Tomasi, J.; Persico, M. *Chem. Rev.* **1994**, *94*, 2027–2094. (b) Simkin, B. Y.; Sheikhet, I. *Quantum Chemical and Statistical Theory of Solutions—A Computational Approach*; Ellis Horwood: London, 1995.

(33) (a) Cancès, M. T.; Mennucci, V.; Tomasi, J. *J. Chem. Phys.* **1997**, *107*, 3032–3041. (b) Cossi, M.; Barone, V.; Cammi, R.; Tomasi, J. *Chem. Phys. Lett.* **1996**, *255*, 327–335. (c) Barone, V.; Cossi, M.; Tomasi, J. *J. Comput. Chem.* **1998**, *19*, 404–417.

## 5. Conclusions

DFT calculations have been used to study the intramolecular Diels–Alder cycloaddition involved in the biosynthesis of paraherquamide A and VM55599. Analysis of the results reveals that these cycloadditions take place through concerted transition structures associated with [4 + 2] processes. The large anti selectivity found for the cycloadditions of the oxindole-based derivatives casts considerable doubt on the construction of the spiro-oxindole framework prior to the cyclization step. In addition, the cycloaddition involving the reduced tertiary amide presents a larger syn selectivity for the formation of the C20 stereogenic center than for the oxidized form. The presence of the C14 methyl in the  $\beta$ -methylproline ring exerts minimal hindrance for the syn approach of the isoprene framework, in agreement with the low facial selectivity found experimentally. Taken as a whole, these results are in reasonable agreement with the available experimental data.

An analysis of the electrophilicity of the reactants involved in these cycloadditions permits an explanation for the low reactivity of these 2-azadienes with nonactivated dienophiles. These cycloadditions thus appear to be associated with concerted [4 + 2] processes. The analysis of the activation parameters for synthetic models of the inter- and intramolecular cycloadditions furnishes a rationalization for a spontaneous (i.e., nonenzyme-catalyzed) cyclization process in the biosynthesis of the VM55599 and paraherquamide. Both the folding of the precursor in the active site of the putative oxidase that forms the azadiene system from the diketopiperazine precursor and the decrease of the low negative entropy of activation for the intramolecular cycloaddition can thus be invoked to account for the feasibility of these biosynthetic cycloadditions.

**Acknowledgment.** This work was supported by research funds provided by the Ministerio de Educación y Cultura of the Spanish Government by DGICYT (Project PB98-1429 to L.R.D.) and the National Institutes of Health (Grant CA70375 to R.M.W.). All calculations were performed on a Cray-Silicon Graphics Origin 2000 of the Servicio de Informática de la Universidad de Valencia. We are most indebted to this center for providing us with computer capabilities.

**Supporting Information Available:** Table with total and relative energies for the stationary points corresponding to the cyclization of 2-azadienes **5**, **11**, **14**, **17**, and **20** at the different computational levels; table with total and relative energies for the reactants and TSs corresponding to the intermolecular cycloaddition between the 2-azadiene **23** and cyclopentene **24** and the cyclization of the 2-azadiene **26**, in the gas phase and in tetrahydrofuran; figure with the HF transition structures corresponding to the cyclization of the oxindoles **11** and **14**; and total energies, imaginary frequencies, and Cartesian coordinates for all stationary points. This material is available free of charge via the Internet at <http://pubs.acs.org>.

JO020564G